Chem. Listy *92,* 1020 - y (1998)

ELECTROPHORETIC SEPARATIONS OF UNIFORMLY CHARGED POLYELECTROLYTES

JAN SUDOR* **and MILOS V. NOVOTNY**

Chemistry Department, Indiana University, Bloomington, Indiana 47405, USA

Received September19, 1997

1. Introduction

1.1. Shape of Macromolecules vs. External Forces

Based on their shape, macromolecules can roughly be divided into three different groups: compact spheres, rigid rods and flexible random coils (shown in the corners of a hypothetical Haug triangle[1]; Fig. 1).

1.1.1. Hydrodynamic Flow

The drag force, F, exerted by a hydrodynamic flow on compact spheres and random coils is Stokes-like, and such macromolecules are practically impermeable to this flow[2]. Consequently, their frictional coefficients, f, are also Stokes-like, i.e., is proportional to a sphere's radius, R, or radius of gyration, R_g, for random coils. (Note that $R_g \sim L^{1/2}$ for an ideal chain and $R_g \sim L^{\sim 0.6}$ when excluded volume effects are not neglected; L is the polymer length). On the other hand, the frictional coefficient of a rigid rod, experiencing a hydrodynamic flow, is simply proportional to the polymer length, L.

1.1.2. Free Electrophoresis

Electrophoresis, in general, describes a mass transport of charged species in an electric field. The separation capability of electrophoresis is based on recognition of the differences in electrophoretic mobilities of charged species. The electrophoretic mobility is proportional, in a simple picture, to the ratio of the effective ion charge to its friction. In contrast to the hydrodynamic flow, the frictional coefficient of a uniformly charged random coil (with $L \gg \kappa^{-1}$, where κ^{-1} is **thickness** of the Debye layer) becomes proportional to its length L in free electrophoresis. Noting that scaling of the frictional coefficients for rigid rods does not change (i.e., $f_{rod} \sim L$). The reason why f_{coil} becomes proportional to L is that the electric force that acts on the **counterions** surrounding the polyelectrolyte is transmitted to the backbone of the chain by viscous shearing and, therefore, cancels locally the long-range component of the flow created by the electric force acting directly on the charged monomer units (i.e., it cancels the hydrodynamic interactions between monomer units). In other words, the electroosmotic flow penetrates a random coil and exerts equal drag on each monomer unit, thus making its charge-to-friction ratio size-independent. Consequently, no deformation of a flexible random-coil in ideal electrophoresis is expected[2,3]. Along the same lines, the electrophoretic mobility of a compact sphere (with $R \gg \kappa^{-1}$) depends only on the sphere's charge density or the zeta potential.

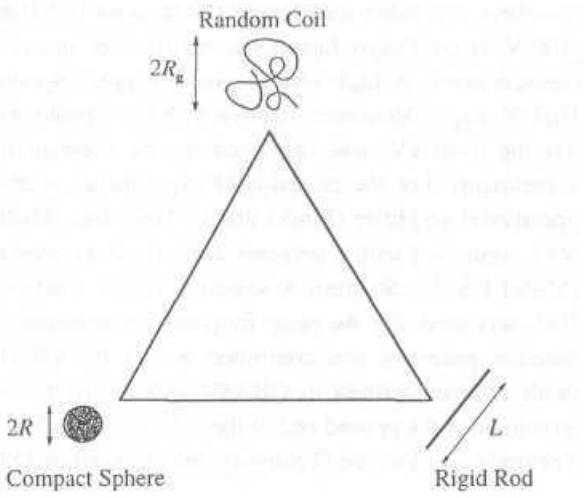

Fig. 1. **Haug triangle representation of the gross conformation of polymers. Adapted from ref.[1]**

* Present address: Institut Curie, Section de Recherche, Laboratoire PCC, 11 Rue Pière et Marie Curie, 75231 Paris Cedex 05, France

The aim of this paper is to describe two different strategies to the separations of uniformly charged polyelectrolytes by means of electrophoresis. First, we will describe an "end-label free-solution electrophoresis" (ELFSE) approach[4,5], where an additional charge or friction, due to an end-label, is formed on the solute. The ELFSE strategy will be demonstrated with uniformly charged, rigid-like oligosaccharides derived from a partialy hydrolyzed *kappa* carrageenan. In a second approach, sieving media (e.g., entangled solutions of linear polymers), under constant or pulsed-field conditions, will be shown to restore the sizing selectivity in the separation of uniformly charged polymers, such as poly(styrene sulfonates) (PSS) and DNAs.

2. Experimental

2.1. Apparatus

A home-built capillary electrophoresis (CE) system was used in all experiments. On-column fluorescence measurements were carried out with a He-Cd laser (Model 56X, Omnichrome, Chino, CA; 5-mW output power at 325 nm) and an argon-ion laser (Model 543, Omnichrome, Chino, CA; 2-mW output power at 488 nm). Signals were isolated by long-pass, low-fluorescence filters ($\lambda_{cut\text{-}off}$ > 490 nm or 550 nm) (Oriel, Stradford, CT) and monitored with a R928 photomultiplier tube (Hamamatsu Photonics K.K., Shizuoka Prefecture, Japan). In the case of UV/VIS absorption detection, a variable-wavelength UV detector (UV1DEC--100-V; Jasco. Tokyo, Japan) was modified for on-column measurements. A high-voltage power supply (Spellman High Voltage Electronics, Plainview, NY), capable of delivering 0–40 kV, was employed for the constant field experiments. For the pulsed-field experiments, a 20-kV operational amplifier (Model 20/20; Trek, Inc., Medina, NY), controlled with a programmable function generator (Model DS340, Stanford Research Systems, Sunnyvale, CA), was used. For the ramp frequency experiments, the function generator was controlled with a PC 486-DX2 (with software written in QBASIC). Wave forms were monitored at the ground end of the column with a 5103 N Tektronix oscilloscope (Tektronix, Inc., Beaverton, OR).

2.2. Chemicals

Citric acid was purchased from EM Science (Cherry Hill, N.J.), sodium hydroxide, hydrochloric acid and phosphoric acid from Fisher Scientific (Fair Lawn, N.J.), and acetic acid (glacial) and boric acid from Mallinckrodt (Paris, KY). Trizma base (tris(hydroxymethyl)aminomethane), EDTA, acrylamide, ammonium persulfate, ethidium bromide, *kappa* carrageenan, and D-glucose-6-sulfate were received from Sigma (St. Louis, MO), and sodium cyanoborohydride from Aldrich (Milwaukee, WI). 8-Aminonaphthalene-1,3,6-trisulfonic acid (ANTS) and 6-aminoquinoline (6-AQ) were the products of Molecular Probes, Inc. (Eugene, OR). The linear polyacrylamide (M_w ~ $5–6.10^6$) and poly(styrenesulfonate) standards (PSS) with the molecular weights of 400,000, 780,000, and 1,132,000, were obtained from Polysciences, Inc. (Warrington, PA). PSS were characterized for their polydispersity (M_w/M_n) through size-exclusion chromatography by the manufacturer ($M_w/M_n \leq 1$ to 1.1), and were reported as nearly 100 % sulfonated. The DNA size standards (DNA concatamers, 4.85-97 kb; and 8.3-48.5 kbp, a mixed digest of λDNA) were a gift from Bio-Rad Laboratories (Hercules, CA), while a monodisperse λDNA (48.5 kb) sample was purchased from New England Biolabs (Beverly, MA).

2.3. Sample preparation

A partially hydrolyzed *kappa* carrageenan and D-glucose-6-sulfate were derivatized through the Schiff-base formation between the aromatic amine of a reagent and the aldehyde form of a sugar, followed by reduction of the Schiff base to a stable product. The reagents concentrations were 30-70 mM in 3 % (w/w) acetic acid; 10 mg sugar was dissolved in 1 ml 0.1-M HCl and mixed with 100 µl reagent. The mixture was heated to 95 °C for 2 minutes before adding 50 µl 2 M sodium cyanoborohydride and then derivatized at 95 °C for 3 hrs. The samples were stable when stored at -20 °C.

3. Results and discussion

3.1. ELFSE of the Oligosaccharides Derived from *kappa*-Carrageenan

To explain the principle of ELFSE model, consider a mixture of uniformly charged polyelectrolytes which are polydisperse in size. Then, an addition of any constant friction, or a constant charge to the components of a mixture will alter the "charge-to-friction" ratio for a smaller solute always more significantly than for a larger one. Let us

assume that the electrophoretic mobility and the frictional coefficient of a polyelectrolyte chain (without an end-label) are μ_0 and f_0, respectively, and the electrophoretic mobility and the frictional coefficient of an end-label are μ_{EL} and f_{EL}, respectively. Under the action of an electric field, E, a free polyelectrolyte chain tends to move with the velocity v_0 ($v_0 = \mu_0 E$) and the end-label with velocity v_{EL} ($v_{EL} = \mu_{EL} E$). In the case when $v_0 > v_{EL}$, the polyelectrolyte chain feels a "breaking" force F_0 from the end-label and the end-label feels a "pulling" force F_{EL} from the polyelectrolyte chain. The situation is reversed when $v_0 < v_{EL}$. Total velocity of the end-labeled solute, v_T, is derived, within the limits of low electric fields when the coupled electro-hydrodynamic equations can be linearized, by superposition of the non-electric(i.e., hydrodynamic) force ($F \neq 0$, and $E = 0$) and the electric force ($F = 0$, and $E \neq 0$)[4]. With the above assumptions, the following force balance equation can be written for the solute[2,3,5,6]:

$$F_0 = f_0 (v_T - \mu_0 E) \quad (1)$$

A similar force balance equation can be set for the end label that feels the pulling force F_{EL} from the solute:

$$F_{EL} = f_{EL} (v_T - \mu_{EL} E) \quad (2)$$

Subsequently, the total velocity v_T of the end-labeled chain can be obtained, self-consistently, by writing the force balance equation for each object of the chain and adding them together, such as:

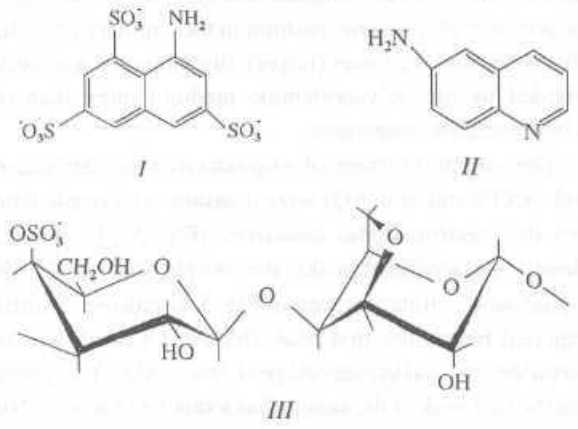

Fig. 2. **Structures of (/) 8-aminonaphthalene-1,3,6-trisulfonic acid (ANTS), (//) 6-aminoquinoline (6-AQ), and (*III*) a *kappa* carrageenan disaccharide unit**

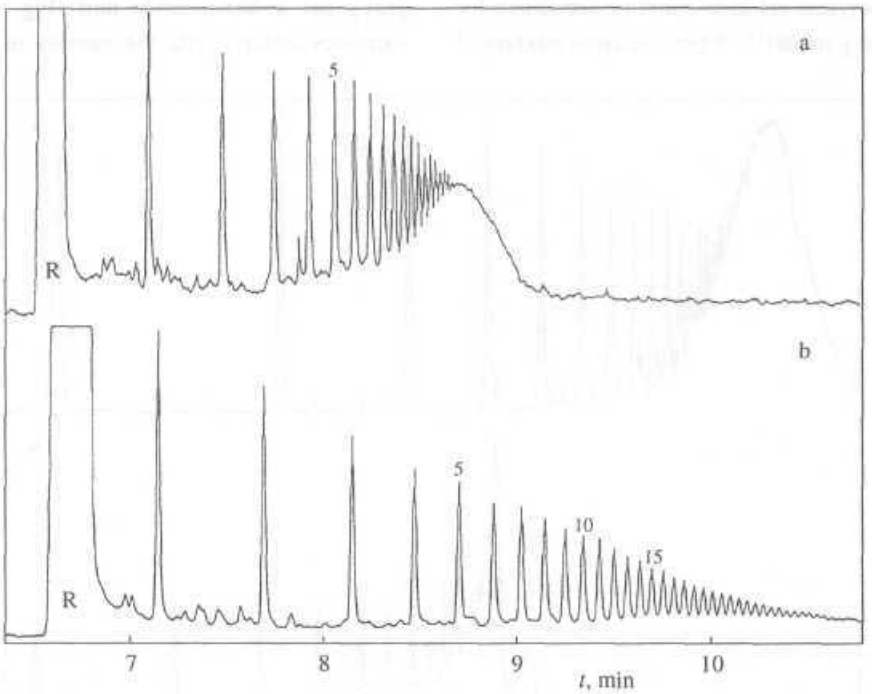

Fig. 3. **Separation of the ANTS-derivatized oligosaccharides derived from a partially hydrolyzed fcappa-carrageenan.** Numbers 5 and 10 above the peaks correspond to deca- and eicosasaccharide, respectively. Capillary: 60-cm effective length (70-cm total); 50-μm i.d. (363-μm o.d.); coated with a linear polyacrylamide. Fluorescence detection (325/>490 nm). (a) Buffer: 25-mM sodium citrate; pH 3.0; hydrodynamic injection: /) = 10 cm, injection time, 10 sec; (b) 25-mM sodium citrate; pH 3.0; 1 %-linear polyacrylamide (Mw ~ 5-6.106); electrokinetic injection: 10 sec. at 100 $V.cm^{-1}$. Applied Voltage: 350 $V.cm^{-1}$ (24 kV). Adapted from ref.[7]

$$F_0 + F_{EL} = 0 \quad (3)$$

Hence,

$$v_T/E = \mu_T = (\mu_0 f_0 + \mu_{EI}\, fa) \,/\, (f_0 + f_{EL}) \quad (4)$$

Equation *(4)* holds for the case when conformations of the polyelectrolyte and the end label do not change during the migration, i.e., it is valid for rigid molecules[5,9].

In order to demonstrate the ELFSE approach, we have chosen a mixture of uniformly charged oligosaccharides derived from faappa-carrageenan, and two "end labels" with different charge-to-friction ratios; *(a)* 8-aminonaphthalene-1,3,6-trisulfonic acid (ANTS)[10], that increases the charge-to-friction ratio of the solute molecules, and *(b)* 6-aminoquinoline (6-AQ)[11] that decreases this ratio (Fig. 2).

The separation of oligomers from the partially hydrolyzed *kappa*-carrageenan derivatized with ANTS is shown in Fig. 3. It is clearly seen that the migration order proceeds from smaller to larger oligomers, and that the separation of larger oligosaccharides is improved in the polymer solution (Fig. 3b) in comparison to the free-buffer condition (Fig. 3a). This is a well-known phenomenon, as the separation mechanisms in a polymer solution could be accounted for by the Ogston sieving model[12]. When the same mixture of sulfated oligosaccharides was derivatized with a slightly positively charged (at pH = 3) reagent (6-AQ), the migration order proceeds from large oligomers (the unresolved "hump" at the beginning) to smaller ones (Fig. 4). This occurs because the reagent has decreased the charge-to-friction ratio of the small oligomers significantly more than for the larger mixture components. Consequently, the resolution between larger oligosaccharides deteriorates upon the presence of a sieving medium in the capillary (Fig. 4b). This is because the faster (larger) oligomers are now being retarded by the polyacrylamide medium more than the slower (smaller) oligomers.

The migration times of oligosaccharides (derivatized with ANTS and/or 6-AQ) were measured and recalculated into the electrophoretic mobilities (Fig. 5). In order to identify the separated peaks, the sample was spiked with D-glucose-6-sulfate. As seen in Fig. 5, D-glucose-6-sulfate migrated before the first peak (for ANTS label) and between the first and the second peak (for 6-AQ). This proves that the first peak of the sample has a smaller charge-to-friction ratio than **the** monosaccharide with one negative charge. Moreover, it is known from the literature[13] that the to/;/?a-carrageenan contains approximately one sulfate group per a disaccharide unit (Fig. 2), and the charge increases linearly with the number of disaccharide units.

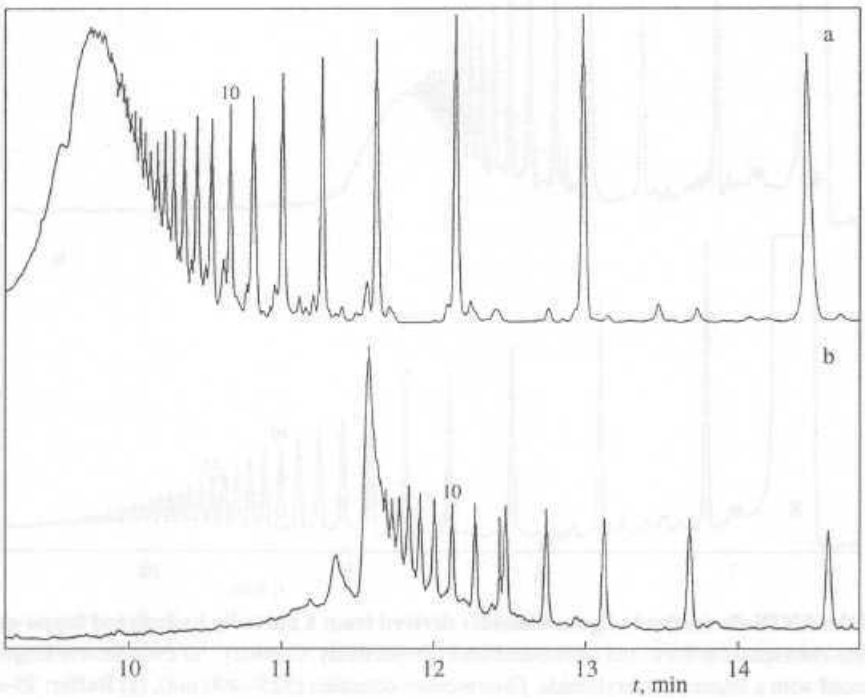

Fig. 4. **Separation of 6-AQ-derivatized oligosaccharides dcrived from a partially hydrolyzed fcappa-carrageenan.** Conditions were the same as in Fig. 3. Adapted from ref.[7]

Consequently, it seems plausible that the first peak in the sample is a disaccharide, and that disaccharide (with one sulfate group) behaves as a monomer unit.

An important parameter for ELFSE model that can be obtained experimentally is the μ_0-value. We have estimated μ_0 from the migration time of the unseparated "hump" (Fig. 5: $\mu_0 = 31.93 \times 10^{-5}$ [$cm^2.V^{-1}.s^{-1}$] +/- 3.1 %). To be able to calculate ν_T as a function of N (where N is the total number of monomers), we must rewrite equation *(4)* into a following form:

$$\nu_T/E = \mu_T = \mu_0 \, (N + \mu_{EL} f_{EL}/\mu_0 f_0^*) \, / \, (N + f_{EL}/f_0^*) \qquad (5)$$

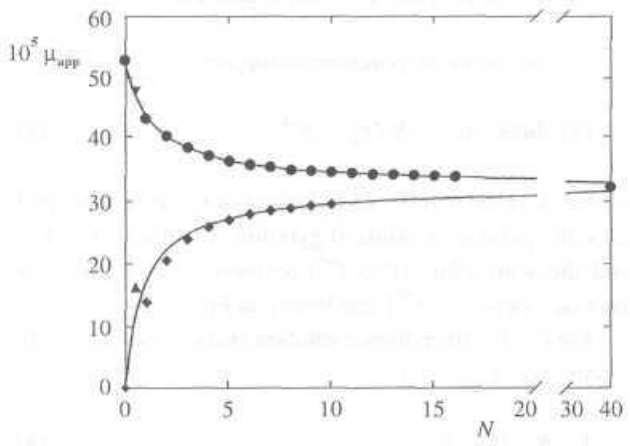

Fig. 5. **Dependence of the electrophoretic mobility** (μ_{app} ($cm^2.Vs^{-1}$)) **on the monomer unit number** (N) **of oligosaccharides derived from a partially hydrolyzed *kappa*-carrageenan. Capillary: effective** length 30 cm (40 cm total). **Buffer:** 25 mM tris-acetate (pH 8.1); Applied voltage: 400V.cm^{-1} (16 kV). ANTS--derivatized oligosaccharides (•); 6-AQ-derivatized oligosaccharides (•); the lines are the calculated values using equation (5); D-glucose-6-sulfate derivatized with either ANTS (T), or 6-AQ (A); μ_0 is shown for N = 40. Adapted from ref.[7]

where f_0^* is the friction of unlabeled monomer unit. The electrophoretic friction of the end-label relative to that of monomer unit (f_{EL} / f_0^*) was calculated from[7,9]

$$f_{EL} / f_0^* = N \, (\mu_0 - \mu_T) / (\mu_T - \mu_{EL}) \qquad (6)$$

for the fifth, seventh and tenth peaks for both pH-values and both end-labels (ANTS and 6-AQ).

Consequently, experimental data (Fig. 5 at pH 8.1 and Fig. 6 at pH 3.0) were fitted by equation (5) (the points are experimental data and the lines are the corresponding calculated mobilities). The values of μ_0 are indicated for a large N (N = 40) (Fig. 5). We observe a rather good

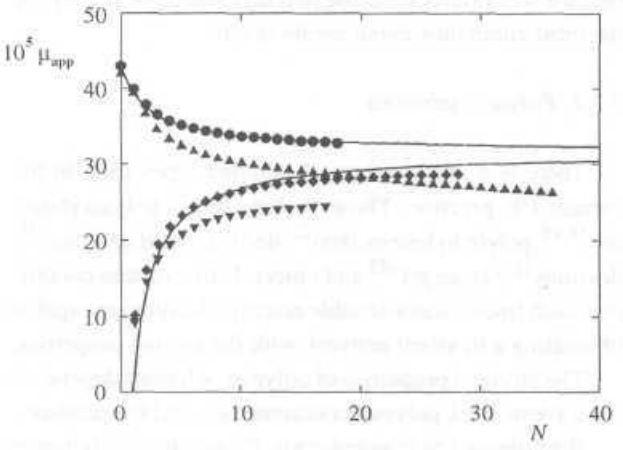

Fig. 6. Dependence of the electrophoretic mobilities (μ_{app} ($cm^2.Vs^{-1}$)) **on the monomer unit number** (N) **of the oligosaccharides derived from a partially hydrolyzed feappa-carrageenan.** ANTS-derivatized oligosaccharides (●); 6-AQ-derivatized oligosaccharides (•); conditions were the same as in Fig. 3a. Corresponding lines are the calculated values using equation (5). The ANTS-derivatized oligosaccharides (A) or 6-AQ-derivatized oligosaccharides (•); conditions were the same as in Fig. 3b. Adapted from ref.[7]

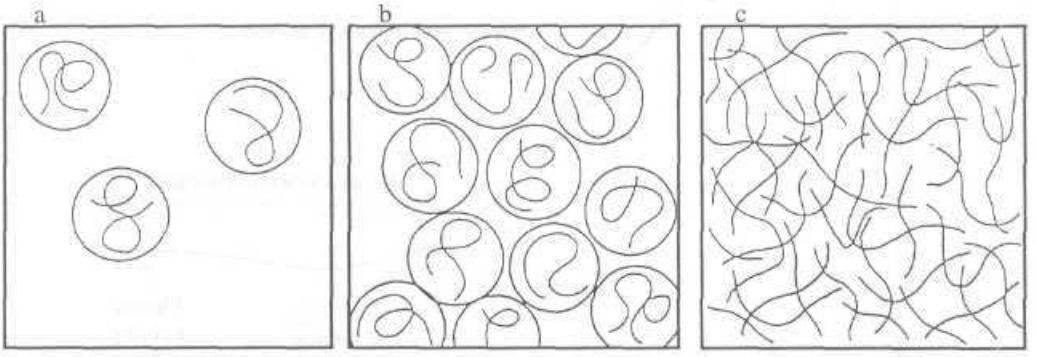

Fig. 7. **Crossover between the dilute and semi-dilute polymer solutions**: (a) dilute ($C < C^*$); (b) overlap threshold ($C \sim C^*$); and (c) semi-dilute ($C > C^*$)

agreement between our experimental data and the mobilities calculated from the ELFSE model (Fig. 5 and 6).

3.2. Gel Electrophoresis

The common remedy to the separation problem with uniformly charged coils is to involve sieving media that influence the solutes' frictional properties and thus induce a size-dependent migration.

There are several classes of sieving matrices applicable to the electrophoretic separations. For instance, permanent gels (either chemically or physically crosslinked)[14-17], polymer solutions[18-23], associative gels[24-26], etc. In following, we will briefly describe polymer solutions as they are the most common sieving media in CE.

3.2.1. Polymer solutions

There is a great variety of polymer types used in the current CE practice. These include linear polyacrylamides[18,19], poly(ethylene oxides)[20], derivatives of cellulose[21], dextrans[22], "synergel"[23] and others. Under certain conditions. such linear, water-soluble macromolecules are capable of creating a transient network with the sieving properties.

The physical properties of polymer solutions depend on the solvents used, polymer concentrations, and temperature.

With respect to concentration C (weight of a polymer per unit volume) of polymer solutions, we can recognize three different regimes: (*a*) dilute; *(b)* semi-dilute; and (c) concentrated. In the dilute regime, the polymer chains are hydrodynamically isolated from each other. A polymer chain occupies a spherical region with its radius of gyration R_g and behaves essentially as a hard sphere. This behavior is driven by the enthalpy considerations, as many "unfavorable" contacts between the chains are needed when they penetrate each other. As the concentration of polymer solution increases, the polymer chains start to overlap with each other. In other words, they become "entangled". An important parameter to differentiate between these two regimes (dilute and semi-dilute) is the so-called overlap threshold concentration C^* (g.ml^{-1}). In other words, C^* is the concentration which is comparable to the concentration inside a single polymer coil, and is given as[27]

$$C^* = (\text{number of monomer units/coil}) / / (\text{volume/coil}) \sim N / R_g^3 \sim N^{-4/5} \quad (7)$$

where, N is the number of monomer units per a chain and R_g is the polymer's radius of gyration. The dilute ($C < C^*$) and the semi-dilute *($C > C^*$)* regimes, with a crossover between them ($C \sim C^*$), are shown in Fig. 7.

For $C > C^*$, the polymer solution creates a network with a pore size, S (Ref.[27]):

$$S \sim R_g (C/C^*)^x \quad (8)$$

Since $R_g \sim N^{3/5}$ and $C^* \sim N^{-4/5}$, S becomes proportional

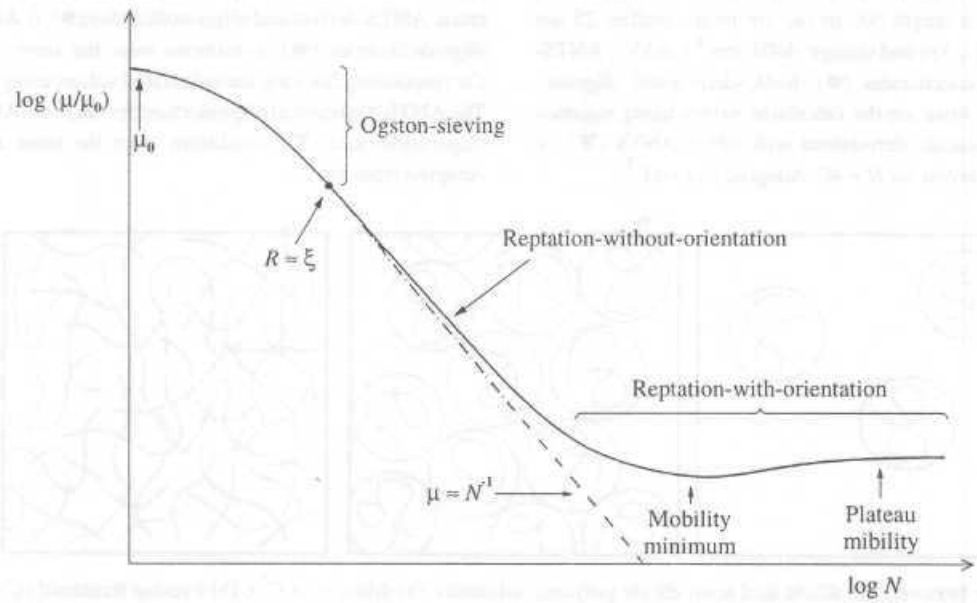

Fig. 8. **Double logarithmic plot of reduced mobility,** μ/μ_0, versus **molecular** size N

to $C^{-3/4}$ (Ref.[27]). Importantly, the pore size of an entangled polymer solution does not depend on a polymer size but only on its concentration, C.

In the following text, electrophoretic separations of flexible polyelectrolytes in entangled polymer solutions (C> C*) will be described under constant and pulsed-field conditions.

3.2.2. Constant-Field Gel Electrophoresis

Three different migration regimes of flexible polyelectrolytes migrating through a sieving medium are shown in Fig. 8. First, the mobility of small solutes ($R_g < S$) exponentially decreases with the molecular radius, R_g. This regime is known as the Ogston sieving regime[12]. Large polyelectrolytes ($R_g > S$) start to reptate through a gel network with the mobility proportional to $1/N$, i.e., such solutes migrate in the so-called "reptation-without-orientation regime"[28-30]. When the molecular size or field strength are further increased, polyelectrolyte chains become field-oriented and start to migrate in the "reptation-with-orientation regime", i.e., with a size-independent mobility[28"30]. Solutes laying between the reptation-without-orientation and reptation--with-orientation regimes migrate through a gel with minimum mobility[29,30].

When electrophoresis of the three poly(styrene sulfonate) (PSS) standards was carried out in an entangled polymer matrix (0.6 % hydroxyethylcellulose (HEC)) under the constant-field conditions, the mobilities were strongly dependent on the electric field strength (Fig. 9)[31]. (Note that picric acid was used as an internal mobility standard to account for the temperature effects on PSS mobilities at different field strengths). A measurable increase in mobilities of the two large PSS was observed in the region between 50-200 V.cm"[1] (Fig. 9). The higher-M_w polymers at first migrated as distinct zones at low voltages, but started to co-migrate at high field-strength values ($E > 200$ V.cm"[1]). In addition, Fig. 10 shows that resolution of the two high-M_w mixture components worsens appreciably at high voltages. The general trends seen in the curve plotted in Fig. 9 and the decrease in component resolution (Fig. 10), as the electric field strength is increased, can be ascribed to the orientation of PSS chains in the direction of the applied field[28-30]. This same trend can be seen from the double

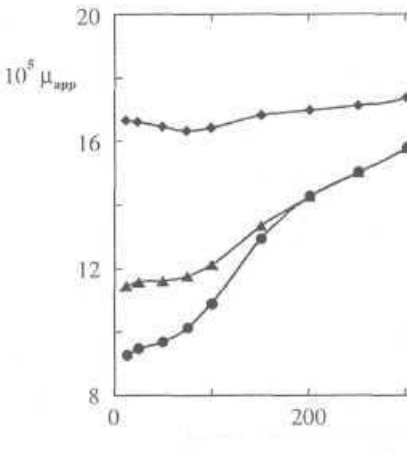

Fig. 9. Dependence of the electrophoretic mobilities (μ_{app} ($cm^2.Vs^{-1}$)) of three PSSs on electric field strength (E ($V.cm^{-1}$)). Conditions: capillary, i.d. 75 μm, total length 40 cm (effective length 20 cm), coated with linear polyacrylamide, and filled with 0.6 % HEC; buffer, 25 mM sodium phosphate, pH 3.0; electromigration injection, 5 sec (25 $V.cm^{-1}$); PSS standards; (•) 400,000, (A) 780,000, and (•) 1,132,000 Da. Adapted from ref.[31]

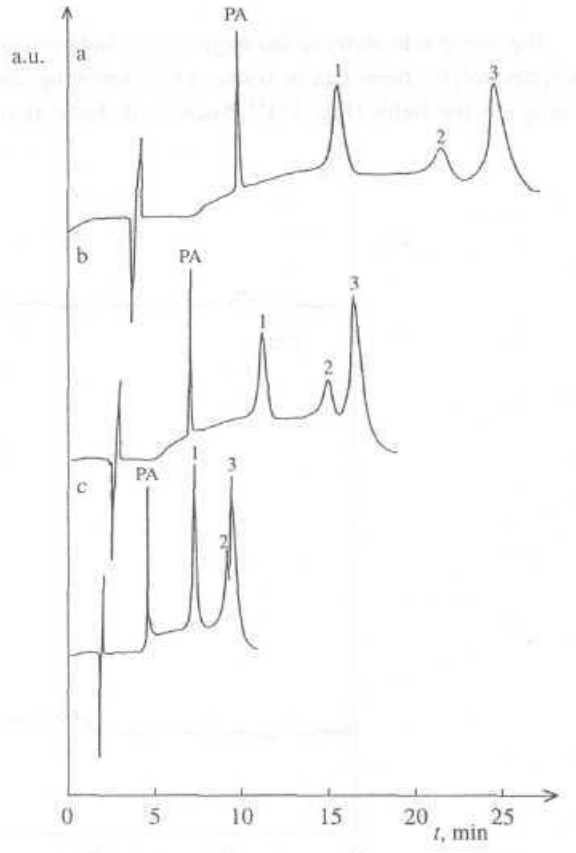

Fig. 10. Separation of PSSs by a continuous field electrophoresis at three different electric field strengths. Peak assignments: PA, picric acid; 1, PSS (M_w 400,000); 2, PSS (M_w 780,000); 3, PSS (M_w 1,132,000); electric field strength, (a) 75 V.cm"', (b) 100 $V.cm^{-1}$, (c) 150 V.cm"'. UV-absorbption detection (254 nm). Other conditions were the same as in Fig. 9. Adapted from ref.[31]

logarithmic plot of mobility VÍ. molecular size (Fig. 11). The line with the slope equal to -1 in Fig. 11 indicates the reptation-without-orientation regime ($\mu/\mu_0 \sim N^{-1}$). However, **the** slope of the line at 12.5 V.cm^{-1} is approximately -0.5, which is one half of the value predicted by the reptation model[28-30]. This result suggests that the reptation **is** not the principal migration mechanism for the two largest PSS standards at the field strength of 12.5 V.cm^{-1}. For instance, local rupture of the polymer network due to a migrating, U-shaped solute or the formation of hairpins on the **end** of an I-shaped solute could explain such a low (absolute) value of the slope (Fig. 11). The onset of the plateau mobility (the reptation-with-orientation; $\mu/\mu_0 \sim N_0$) for two largest PSS can be clearly seen above 150 V.cm^{-1} (Fig. 11).

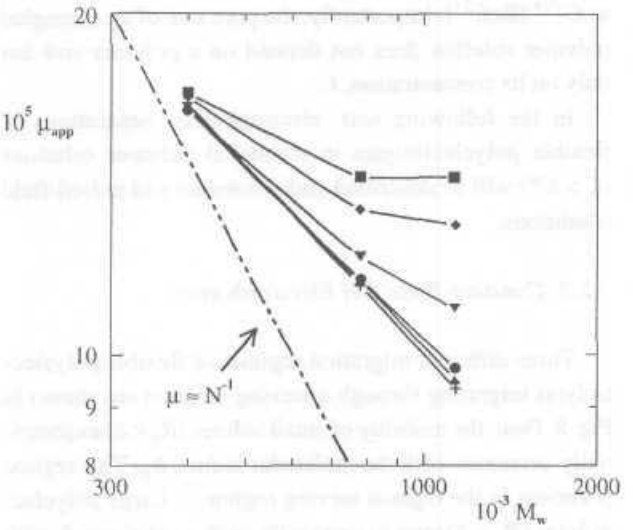

Fig. 11. **Log-log dependence of the electrophoretic mobilities (μ_{app} (cm^2.Vs^{-1})) on molecular weight (M_w) for three PSSs.** Electric field strength: (+) 12.5 V.cm^{-1}, (A) 25 V.cm^{-1}, (•) 50 V.cm^{-1}, (T) 100 V.cm^{-1}, (•) 150 V.cm^{-1}, and (•) 250 V.cm^{-1}. Other conditions were the same as in Fig. 9. Adapted from **ref.**[31]

3.2.3. *Pulsed-Field Gel Electrophoresis*

The sizing selectivity in the migration of field oriented polyelectrolyte chains can be restored by employing alternating electric fields (Fig. 12)[32]. Such fields force an ori-

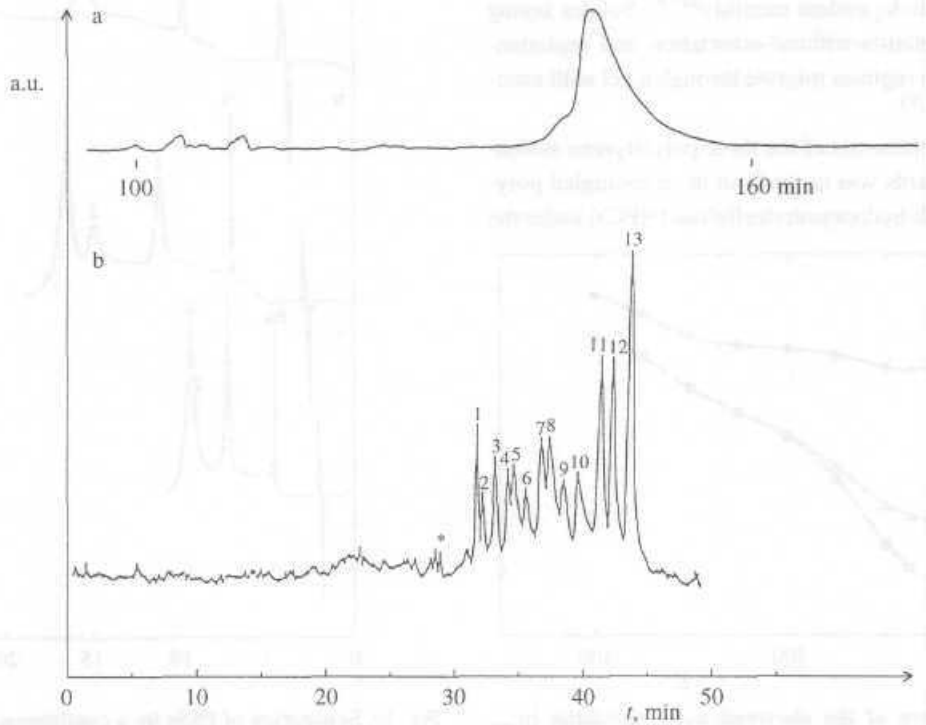

Fig. 12. **Separation of the 8.3–48.5 kbp DNA size standards under (a) constant field and (b) pulsed-field capillary electrophoresis.** Peak assignments: 1, 8.3 kbp; 2, 8.6 kbp; 3, 10.1 kbp; 4, 12.2 kbp; 5, 15.0 kbp; 6, 17.1 kbp; 7, 19.4 kbp; 8, 22.6 kbp; 9, 24.8 kbp; 10, 29.9 kbp; 11,33.5 kbp; 12, 38.4 kbp; and 13, 48.5 kbp; the circle indicates two bands (1.1 kbp, and 1.5 kbp; not identified). Experimental conditions: buffer: 0.5 x TBE (44.5 mM Tris, 44.5 mM **boric** acid, and 1.25 mM EDTA), pH 8.1, 0.6 % linear polyacrylamide (M_w - 5–6.10^6); UV-absorbption detection (260 nm); electromigration injection, 30 sec (25 V.cm^{-1}); applied voltage, 25 V.cm^{-1} for (a); E_{dc} = -50 V.cm^{-1}, and E_{sin} = 100 V.cm^{-1} for (b); frequency of the applied sine-wave input signal: 12 Hz. Adapted from ref.[32]

ented chain to reorient in a new field direction, while the reorientation time is size dependent. The reorientation time (also called reptation time, t_{rep}) is the time required for a DNA molecule to move over a distance equal to its lenth, and is given as[28-30,33]

$$t_{rep} \sim N\langle\cos\phi\rangle / v_{el} \qquad (9)$$

where $\langle\cos\phi\rangle$ is the average chain orientation and v_{el} is the polymer's electrophoretic velocity. If $t_{rep} \sim t_p$ (where t_p is the pulse time; $t_p = /p + t_B$, with t_F being the duration of the forward and t_B of the backward pulse, respectively), the alternating field will have the strongest effect on the DNA velocity. For $t_{rep} / t_p \ll 1$, the DNA molecule will have a sufficient time to orient itself in both directions, migrating most of the time in the reptation-with-orientation regime. Conversely, if $t_{rep} / t_p \gg 1$, the DNA chain will not "feel" the high frequency alternating field, migrating once again with a size-independent velocity that is somewhat smaller compared to the velocity of a DNA migrating in the reptation-with-orientation regime.

Carle et al.[34] demonstrated in their field-inversion gel electrophoresis (FIGE) experiment, that a DNA molecule passes through a mobility minimum at a certain t_p. Consequently, Duke and Viovy[35] proposed that a DNA chain will migrate with a minimum mobility in forward direction if the duration of forward pulse, t_F, is equal to the so-called overstretching time, t_{ov}, and $t_B < t_{ov}$. In such a situation, the DNA chain just grows its arms (O → U conformational transition) during the forward pulse, and then retracts them (U → O conformational transition) during the backward pulse, making no overall progress along the gel. The overstretching time was derived analytically by Lim et al.[36] and it scales with the polymer size N and the external electric field E as:

$$t_{ov} \sim N \ln N/E \qquad (10)$$

In order to study the mobility minima in pulsed-field CE, we measured the migration times of 14 DNA fragments (from 5 to 70 kbp, with 5-kbp spacing) as a function of the frequency of external electric field[37]. The double logarithmic dependence of the apparent electrophoretic mobilities on the forward pulse duration is shown in Fig. 13. For the sake of clarity, the apparent mobilities of only eight DNA fragments (10-70 kbp with 10-kbp spacing) is shown in Fig. 13. The electrophoretic mobility of the smallest fragment (5 kbp) was almost constant and was used as an internal mobility standard, while the 10 kbp fragment did not experience any mobility minimum in the range of tested frequencies (from 1 to 30 Hz). It is obvious that the mobility is decreasing (from the right side of a long-pulse duration) until it reaches a minimum (at a longer pulse for the larger DNA molecules and at a shorter pulse for the smaller ones),

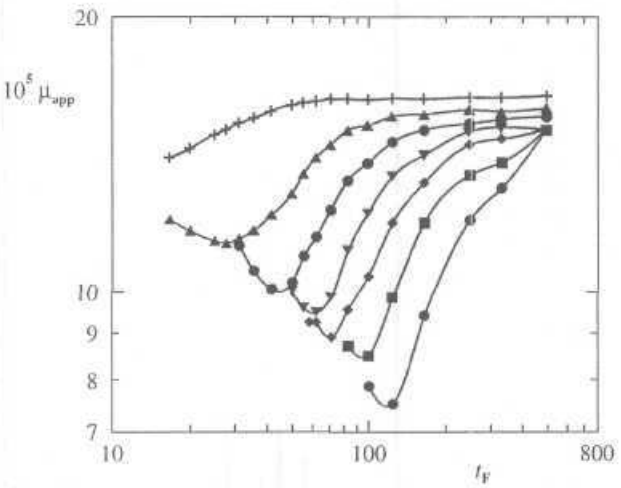

Fig. 13. **Double logarithmic plot of the apparent electrophoretic mobility (μ_{app} (cm^2.V^{-1}s^{-1})) vs. the forward pulse durations, t_F (ms)**, for the DNA molecules, ranging from 10 to 70 kbp ((+) 10-kbp. (A) 20-kbp, (•) 30-kbp, (▼) 40-kbp, (•) 50-kbp, (•) 60-kbp, and (•) 70-kbp). Experimental conditions: Capillary: effective length 15 cm (total length 25 cm); inner diameter 100 μm; the inner capillary surface was coated with a linear polyacrylamide. Fluorescence detection (488/550 nm). Buffer: 1 x TBE buffer (89 mM Tris-borate, 2.5 mM EDTA, pH 8.1 (0.8 %-linear polyacrylamide, $M_w \sim 5\text{-}6.10^6$). Applied Voltage: square-wave electric field, forward pulse –120 V cm^{-1} backward pulse +40 V.cm^{-1}, durations of the forward and backward pulses were equal. Adapted from ref.[37]

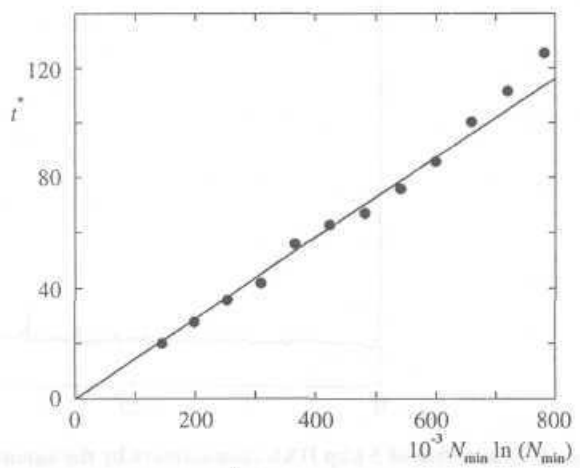

Fig. 14. Dependence of t^* (ms) on the size of DNA molecules N. Conditions were the same as in Fig. 13. Adapted from ref.[37]

with a subsequent tendency to increase again. Duration of the forward pulse at which the mobility minimum appeared was further studied.

Based on the assumption that a **DNA** molecule migrates with a minimum velocity in forward direction when $t_F = t_{ov}$, we used the following equation to fit the experimental data:

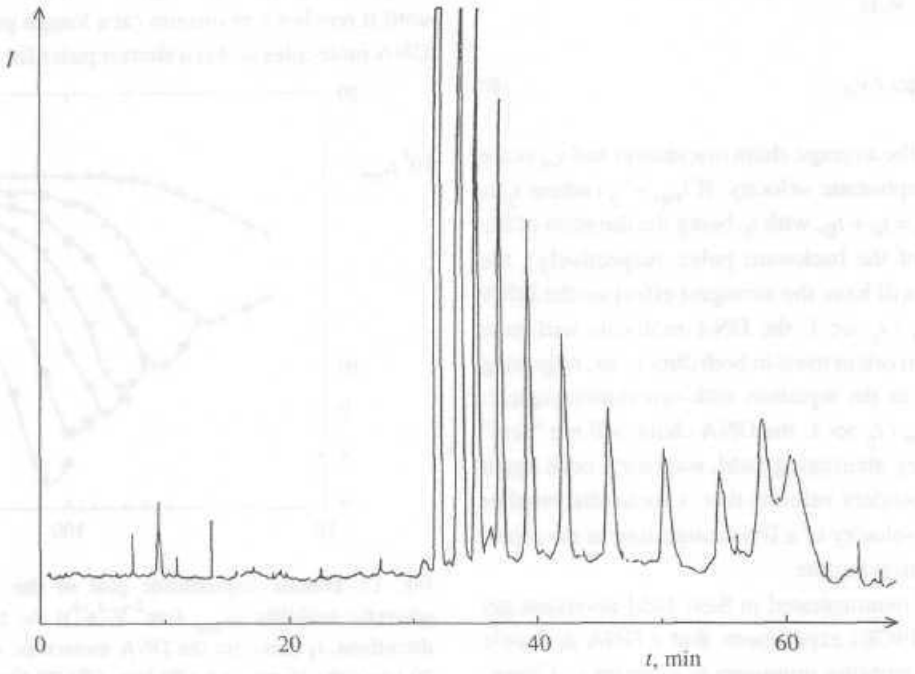

Fig. 15. **Separation of 5 kbp DNA concatamers by a square-wave electric field at a constant frequency of 6 Hz.** Other conditions were the same as in Fig. 13

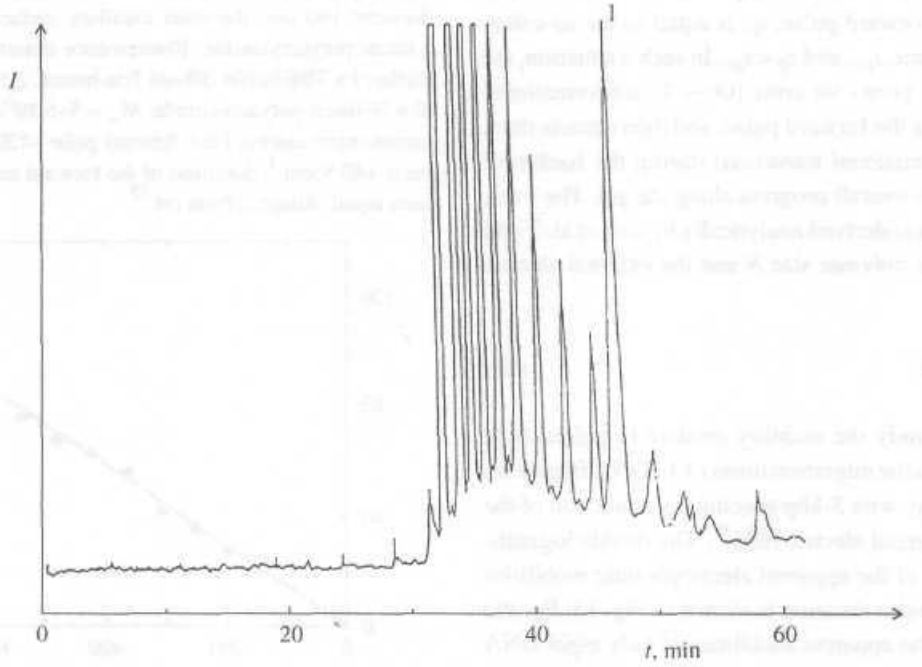

Fig. 16. **Separation of 5 kbp DNA concatamers by the square-wave electric field utilizing a frequency gradient from 7 to 2 Hz, step: 0.001 Hz/0.6** sec, **total time of gradient 50 min.** (1) above the 1 Oth peak indicates a monodisperse lambda DNA molecule (48.5 kbp) added to the sample. Other conditions were the same as in Fig. 13. Adapted from ref.[37]

$$t^* = k\,(N_{min} / E)\,\ln(N_{min})\,C \qquad (11)$$

where t^* is the duration of forward pulse at which a given DNA molecule migrates with the minimum velocity, k is a proportionality constant, N_{min} is the number of basepairs (bp) of a chain migrating with the minimum velocity, E is the electric field strength ($V.m^{-1}$), and C is the concentration of linear polyacrylamide ($g.ml^{-1}$). The proportionality constant was determined for the best fit of the experimental data as k = 2.3 (Fig. 14). The calculated curve fits the experimental data quite well, except for the largest fragments where the times of forward pulses at which the DNA fragments experienced a mobility minimum were longer than those calculated from equation (*11*); this can be due to a more profound deformation of the sieving media by large DNAs. migrating in a U-shape conformation.

The determination of pulse time that influences the DNA mobility the most, for a defined experimental condition, is important from the practical point of view. Through selecting the frequency of applied electric field, one can selectively change the electrophoretic mobility of a DNA chain with a particular size. As an example, the separations of 5kbp DNA concatamers under constant frequency is shown in Fig. 15. It can be clearly seen that the separation window is "open" for a medium sized DNAs, while largest fragments comigrate together. This indicates that the reptation times of the largest DNA molecules were smaller than duration of the forward pulse (at a given field strength). Consequently, these fragments did not have time to respond to the external electric field and migrated with a size-independent velocity. The separation window can, however, be open for all fragments, in a single run, when a ramp of frequency is employed (Fig. 16). Thus, in order to achieve high resolution in a narrow size window, constant frequency protocols should be employed. On the other hand, to increase a separation window for a wider DNA size range, techniques with sweeping or randomly varying frequencies [38,39] can be utilized.

4. Conclusions

The separation of uniformly charged rigid-rods and random-coils by means of electrophoresis requires breaking the symmetry between their charge and friction. We have shown here that this symmetry-breaking can be achieved through the end-labeling strategy and the use of sieving media, e.g., polymer solutions. While the end-labeling scheme is, in principle, unlimited by solute's size, the sieving media could not separate very large, flexible polyelectrolytes that became oriented in the field direction. (Note that in practice the applicability of ELFSE deteriorates with an increasing solute size, since the requirements for large end-labels may become unreasonable, while gel electrophoresis becomes more effective for large solutes, which is a limitation given by the pore size of a gel.) In such circumstances, alternating electric fields were employed that forced the molecules to reorient in a new field direction. The size-selective migrations were reconstructed through the size-dependence in the molecular reorientation time.

REFERENCES

1. Harding S. E.: Biophys. Chem. *55,* 69 (1995).
2. Long D., Viovy J. L., Ajdari A.: Biopolymers *39,* 755 (1996).
3. Long D., Viovy J. L., Ajdari A.: Phys. Rev. Lett. *76,* 3858(1996).
4. Mayer P., Slater G. W., Drouin G: Anal. Chem. *66,* 1777(1994).
5. Long D., Ajdari A.: Electrophoresis *17,* 1161 (1996).
6. Long D., Viovy J. L., Ajdari A.: J. Phys.: Condens. Matter *8,* 9471 (1996).
7. Sudor J., Novotny M. V.: Anal. Chem. *67,* 4205 (1995).
8. Sudor J., Novotny M. V.: Anal. Chem. *69,* 3199 (1997).
9. Sudor J.: *PhD Thesis.* Indiana University 1997.
10. Chiesa C, Horwath C: J. Chromatogr. *645,* 337 (1993).
11. Nashabeh W., Rassi Z. El.: J. Chromatogr. *600,* 279 (1992).
12. Ogston A. G.: Trans. Farady Soc. *54,* 1754 (1958).
13. Yalpani M.: *Polysaccharides: Synthesis, Modifications and Structure/Property Relations.* Elsevier, Amsterdam 1988.
14. Cohen A. S., Karger B. L.: J. Chromatogr. *397,* 409 (1987).
15. Hjertén S., Elenbring K., Kilar F., Chen A. J. *C,* Siebert C. J., Zhu M. D.: J. Chromatogr. *403,* 47 (1987).
16. Dolnik V., Cobb K. A., Novotny M. V.: J. Microcolumn Sep. *3,* 155(1991).
17. Chen N., Wu L., Palm A., Srichaiyo T., Hjertén S.: Electrophoresis *17,* 1443(1996).
18. Heiger D. N., Cohen A. S., Karger B. L.: J. Chromatogr. *516,* 33 (1990).
19. Heller C, Viovy J. L.: Appl. Theor. Electrophoresis *4,* 39 (1994).

20. Fung E. N., Yeung E. S.: Anal. Chem. *67,* 1913 (1995).
21. Grossman P. D., Soane D. S.: Biopolymers *31,* 1221 (1991).
22. Ganzler K., Greve K. S., Cohen A. S.. Karger B. L., Guttman A., Cooke N. C: Anal. Chem. *64,* 2665 (1992).
23. Dolnik V., Novotny M. V.: J. Microcolumn Sep. *4,* 515(1992).
24. Glass J. E. (ed.): *Polymers in Aqueous Media: Performance Through Association,* Advances in Chemistry 223. American Chemical Society, Washington DC 1989.
25. Shultz D. N., Glass J. E. (ed.): *Polymers as Rheology Modifiers,* Advances in Chemistry 462, American Chemical Society, Washington DC 1991.
26. Menchen S., Johnson B., Winnik M. A., Xu B.: Electrophoresis *17,* 1451 (1996).
27. de Gennes P. G.: *Scaling Concepts in Polymer Physics.* Cornell University Press, Ithaca 1991.
28. Lumpkin O. J., Dejardin P., Zimm B. H.: Biopolymers *24,* 1573(1985).
29. Slater G. W., Noolandi J.: Phys. Rev. Lett. *55,* 1579 (1985).
30. Duke T. A. 1, Viovy J. L., Semenov A. N.: Biopolymers *34.* 239 (1994).
31. Sudor J., Novotny M. V.: Anal. Chem. *66,* 2139 (1994).
32. Sudor J., Novotny M. V.: Anal. Chem. *66,* 2446 (1994).
33. Heller C., PakiezaC, Viovy J. L.: Electrophoresis *16,* 1423(1995).
34. Carle C. F., Frank M., Olson M.: Science *232,* 65 (1986).
35. Duke T. A. J., Viovy J. L.: J. Chem. Phys. *96,* 8552 (1992).
36. Lim H. A., Slater G. W., Noolandi J.: J. Chem. Phys. 92,709(1990).
37. Sudor J., Novotny M. V.: Nucleic Acid Res. *23,* 2538 (1995).
38. Heller C, Pohl F. M.: Nucleic Acids Res. *18,* 6299 (1990).
39. Navin M.J., Rapp T. L., Morris M. D.: Anal. Chem. *66,* 1179 (1994).

J. **Sudor and** M. V. **Novotny** *(Chemistry Department, Indiana University, Bloomingto, Indiana 407405, USA):*

Electrophoretic Scparations of Uniformly Charged Polyelectrolytes

Uniformly charged polyelectrolytes migrate with size-independent velocities in free solutions and when only electric forces are present. This is due to a symmetry between the charge of the solutes and friction. To size-separate such polyelectrolytes by means of electrophoresis, this symmetry must be "broken". Two different strategies how to induce size-dependent migrations of uniformly charged polyelectrolytes are shown. First, the solutes charge-to-friction ratio has been altered by an attachment of a suitable hydrophilic end-1abel, modifying thus the electrophoretic mobility of a small solute, in contrast to larger molecules, more significantly. Secondly, solutes frictional properties have been modified through use of sieving media, thus slowing down the large solutes more substantially when compared to small molecules. However, it has also been shown that large and flexible solutes (e.g., poly(styrene sulfonates) and DNAs) start to migrate with size-independent velocities under strong electric fields. This phenomenon is a consequence of the solutes reptative motion through a sieving medium with a subsequent molecular field orientation. Finally, it was demonstrated that alternating (pulsed) fields, that force the solute to reorient in a new field direction, can restore the size-dependent migrations of large flexible polyelectrolytes.